Research Article

Seham S. Alterary* and Anfal AlKhamees

Synthesis, surface modification, and characterization of Fe_3O_4@SiO_2 core@shell nanostructure

https://doi.org/10.1515/gps-2021-0031
received March 02, 2021; accepted April 06, 2021

Abstract: In recent times, nanoparticles have been the focal point of research in nanoscience due to their wide scope of potential applications in all fields of science. Iron oxide (Fe_3O_4) nanoparticles (NPs) show incredible magnetic saturation, stability, biocompatibility, and intuitive properties on the surface, which makes them ideal for being utilized in several ways. In the present study, Fe_3O_4 NPs were synthesized by co-precipitation and further coated with silica (SiO_2) to avoid aggregation. Synthesized nanoparticles (Fe_3O_4@SiO_2) were individually functionalized using glycine and malonic acid and characterized by various spectroscopies and microscopies techniques. XRD diffraction analysis showed that the presence of SiO_2 did not alter the diffraction pattern peaks, which represented the existence of Fe_3O_4. The presence of Fe_3O_4 and SiO_2 nanoparticles were further confirmed using EDS. Transmission electron microscope micrographs of the synthesized nanoparticles exhibited spherical shape and confirmed the increase in particle size after coating with SiO_2. Also, the analysis of dynamic light scattering showed that the particle size of Fe_3O_4@SiO_2 functionalized with malonic acid (229.433 nm) was greater than those functionalized with glycine (57.2496 nm). However, the surface area was greater in Fe_3O_4@SiO_2-glycine (104.8 m^2/g) than Fe_3O_4@SiO_2-malonic acid (26.15 m^2/g). The key findings suggest that the synthesized core-shell Fe_3O_4@SiO_2 nanoparticles are a promising candidate for a wide array of applications in the field of medicine and environmental science.

Keywords: core@shell, Fe_3O_4@SiO_2, functionalization, nanostructure, surface modification

*** Corresponding author: Seham S. Alterary,** Department of Chemistry, King Saud University, Riyadh, Saudi Arabia; King Abdullah Institute of Nanotechnology, King Saud University, Riyadh, Saudi Arabia, e-mail: salterary@ksu.edu.sa
Anfal AlKhamees: Department of Chemistry, King Saud University, Riyadh, Saudi Arabia, e-mail: a-a-k-1415@hotmail.com
ORCID: Seham S. Alterary 0000-0002-4176-2840

1 Introduction

In the recent decade, applications of nanotechnology have emerged with an increasing use of nanosized materials in various fields due to their unique properties at the nanoscale in comparison with their bulk counterparts [1]. Integration of nanotechnology with other sciences has resulted in the rapid development of novel research areas, which will improve and revolutionize technology in several industries [2].

Magnetite and Fe_3O_4 NPs provide a unique nanoplatform and play a major role in providing a broad range of applications owing to their important magnetic property of superparamagnetism. The phenomenon shows that ferromagnetic or ferrimagnetic nanoparticles would have zero magnetic remanence together with a high magnetic susceptibility. Among them, Fe_3O_4 NPs stand out due to their high biocompatibility, low toxicity, strong superparamagnetic property, and easy preparation process, and thus, they have attracted increasing attention [3,4] in the field of research. Fe_3O_4 NPs do have their limitations, such as rapid agglomeration, wide surface area, high chemical reactivity, and high surface energy, resulting in magnetism loss [5]. Therefore, appropriate surface modification of Fe_3O_4 NPs is required to avoid the aforementioned problems. The coating is the most common surface modification method to conjugate organic or inorganic materials onto the surface of iron oxide nanoparticles. This approach avoids not only the oxidation and agglomeration but also provides the possibility of further functionalization [6,7]. Functionalization of magnetic NPs boosts up their physicochemical properties, making them ideal candidates for catalysis or biomedicine purposes [8]. Many studies are conducted on the synthesis of Fe_3O_4 nanoparticles into composite structures with other materials. Chang et al. [9] and Sobhanardakani and Zandipak [10] have reported the formation of silica layers on the surface of stabilized magnetite nanoparticles using a surfactant [11]. Amorphous SiO_2 is the most representative material

among potential candidates for constructing core-shell structures with Fe_3O_4. SiO_2 is used because of its inherent high thermal stability, physicochemical durability, and surface characteristics, which is because it retains a large number of surface hydroxyl groups [12,13]. This offers a mode to overcome the limitations encountered during the synthesis of Fe_3O_4 nanoparticles. Among the methods of synthesis used, chemical co-precipitation is the most common method both for the laboratory purpose and on a larger scale for industrial processes since it is highly advantageous. The process has easy processing operation, high yield product, low temperature, and time of reaction in comparison with methods like thermal decomposition and hydrothermal and utilizes inorganic reactants and environmental-friendly solvents such as water [14]. To make a core-shell structure, there is a major deficiency in using Fe_3O_4 nanoparticles obtained by co-precipitation due to the large surface-to-volume ratio, high surface energy, and magnetic dipole–dipole attractions between the particles, and magnetic nanostructures are highly prone to aggregation. To synthesize well-dispersed silica-coated Fe_3O_4 NPs, sol–gel method, the Stöber method, and microemulsion are the most common methods for coating the surface of Fe_3O_4 nanoparticles with silica [15,16].

With this premise, the present study was carried out to use the Fe_3O_4 nanoparticle as a magnetic core coated by SiO_2 shell and then modified by organic and inorganic reagents to synthesize the Fe_3O_4@SiO_2 as an efficient nanomagnetic catalyst. Initially, the magnetic iron oxide nanoparticles (Fe_3O_4 NPs) were produced using the co-precipitation method and then coated with SiO_2. The coated particles are then functionalized with glycine and malonic acid.

2 Materials and methods

2.1 Co-precipitation method synthesized of Fe_3O_4 NPs

A volume of 500 mL of 1.5 M NaOH (BdH Laboratory Supplies) was added with a dropper with continual stirring at 80°C to the mixture of $FeCl_3{\cdot}6H_2O$ (LOBA Chemie; 0.04 mol, 10.8 g) and $FeSO_4{\cdot}7H_2O$ (UNI-CHEM; 0.02 mol, 5.5 g) dissolved in 50 mL of 0.5 M HCl (Salzsäure rauchend). Thereafter, the prepared Fe_3O_4 precipitant was collected with a magnet, washed several times with deionized water, and dried for 7 h at 50°C [17,18].

2.2 Synthesis of silica-coated Fe_3O_4 NPs (Fe_3O_4@SiO_2 NPs)

A volume of 10 mL of deionized water, 30 mL of absolute ethanol (CH_3CH_2OH ≥99.8%; Sigma-Aldrich), and 1 mL of ammonia (30% NH_3; Applichem Panreac) were added to 0.5 g Fe_3O_4 nanoparticles. This mixture was incubated in an ultrasonic tank for 30 min, after which we added 2.5 mL of tetraethylorthosilicate (TEOS ≥99.0%; Fluka) while stirring for 22 h. The coated Fe_3O_4@SiO_2 was dried at room temperature [19,20].

2.3 Surface modification of Fe_3O_4@SiO_2 NPs by glycine and malonic acid

A total of 0.15 g of Fe_3O_4@SiO_2 NPs was added to 7.5 mL of deionized water in ultrasonic tanks. Then, 0.15 g of glycine (WINLAB) or malonic acid (LOBA Chemie) was added to the solution by stirring at 90°C for 20 min. After the reaction was complete, the precipitate was washed three times with deionized water and dried under vacuum for 12 h at 50°C [21,22].

2.4 Characterization techniques

The FTIR spectra of Fe_3O_4, Fe_3O_4@SiO_2, Fe_3O_4@SiO_2-glycine, and $Fe_3O_4{\cdot}SiO_2$-malonic acid nanoparticles were analyzed by Fourier transform infrared spectrophotometer (Perkin-Elmer Spectrum BX) to examine the functional chemicals groups of the prepared samples using the potassium bromide (KBr) disk method. The structural analyses of the collected samples were carried out using XRD and Bruker D5005 diffractometers using CuK5-007 radiation (5-007 = 1.5418 A_0). The average particle size of the prepared nanoparticles was calculated according to the Scherrer equation. The particle size distribution was investigated by a dynamic light scattering (DLS) technique using a Zetasizer (HT Laser, ZEN3600 Malvern Instruments, Malvern, UK). To determine particle size, morphology, and composition of Fe_3O_4, Fe_3O_4@SiO_2 and acquired samples were examined using a JEOL JSM-6300 SEM with an EDS and a JEM-200CX TEM. The Brunau–Emmet–Teller (BET) method was employed to measure the surface area of Fe_3O_4@SiO_2-glycine and Fe_3O_4@SiO_2-malonic acid nanoparticles with a Micromeritics Gemini 2360 surface area analyzer. Nitrogen gas molecules were

adsorbed onto the solid surface, which allows measurement of the surface area of the nanoparticles.

2.5 Statistical analysis

All experiments were performed in triplicate. Results were expressed as means ± standard deviation (n = 3). The size of nanoparticles was measured from the scanning electron microscope (SEM) and transmission electron microscope (TEM) pictures using ImageJ software.

3 Results and discussion

3.1 FTIR analysis

The chemical compositions of Fe_3O_4, Fe_3O_4@SiO_2, Fe_3O_4@SiO_2-glycine, and Fe_3O_4@SiO_2-malonic acid nanoparticles were characterized using FTIR spectroscopy as shown in Figure 1. The FTIR results confirmed that the nanoparticles were composed of iron oxide; the Fe_3O_4 nanoparticles exhibited well-defined peaks at 577, 974, 1,622, and 3,118 cm^{-1}. The peak at 577 cm^{-1} indicates the presence of the Fe–O bond. This peak was observed in all prepared samples, indicating the presence of Fe_3O_4 nanoparticles in all preparations. The occurrence of a peak of 974 cm^{-1} is due to the presence of the nitrate group. In addition, the peaks at 1,622 and 3,118 cm^{-1} were due to the bending vibration of absorbed water and O–H stretching, respectively [23,24]. The Fe_3O_4@SiO_2 spectrum exhibits specific bands positioned at 1,080, 1,082, 1,400, and 3,141 cm^{-1}. The 1,080 cm^{-1} peak corresponds to Si–O–Si (siloxane) stretching vibrations, while the 1,082 cm^{-1} corresponds to Fe–O–Si stretching vibrations, confirming the presence of SiO_2 layers in the nanoparticles. The low-intensity peak at 1,400 cm^{-1} corresponds to Fe–O stretching, and the band at 3,141 cm^{-1} corresponds to O–H stretching. These results strongly suggested that the Fe_3O_4 nanoparticles were successfully coated with SiO_2 [25,26]. The Fe_3O_4@SiO_2 was loaded with glycine and malonic acid individually, which was also confirmed using FTIR spectroscopy. The functionalization with glycine yielded specific peaks in the Fe_3O_4@SiO_2-glycine sample at 465, 597, 892, 1,030, 1,087, 1,327, 1,406, 1,620, 3,206, and 3,400 cm^{-1}. Carboxylic group peaks appeared at 465, 598, and ~700 cm^{-1}. C–C–N symmetric and asymmetric stretching vibration bands appear at 892 and 1,030 cm^{-1}, respectively. NH_3 rocking and CH_2 twisting bands appeared at 1,087 and 1,327 cm^{-1}, respectively. The band at 1,620 corresponds to CO_2 asymmetric stretching, and the bands at 3,206 and 3,400 cm^{-1} correspond to the O–H stretching vibration and intramolecular C–H stretching vibration, respectively [27]. The malonic acid-specific bands appeared at 956, 1,083, 1,369, 1,564, 1,722, and 3,425 cm^{-1}. The peak at 956 cm^{-1} corresponds to the C–C–C stretching vibration, and the peak at 1,083 cm^{-1} corresponds to CH_2 rocking vibration. The O–H bending and C–O stretching bands appear at 1,369 cm^{-1}. The C═O stretching vibration appears at 1,722 cm^{-1}. Finally, the band at 3,425 cm^{-1} indicates O–H stretching [28–30].

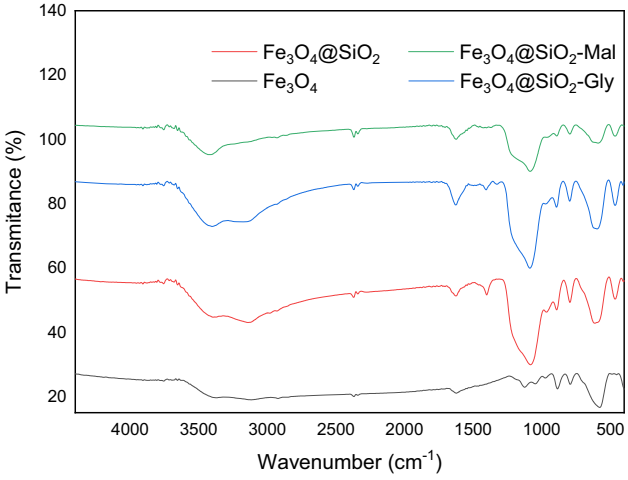

Figure 1: FTIR spectra of the synthesized nanoparticles.

3.2 XRD analysis

The composition of the prepared nanomaterial was primarily identified using XRD. XRD patterns for Fe_3O_4, Fe_3O_4@SiO_2, Fe_3O_4@SiO_2-glycine, and Fe_3O_4@SiO_2-malonic acid are depicted in Figure 2. Peaks at 35.6°, 43.29°, 57.5°, and 62.82° were assigned to (311), (400), (511), and (440) reflections of Fe_3O_4, respectively (Figure 2a) [31,32]. This suggests that the Fe_3O_4@SiO_2 nanoparticles were synthesized successfully without damaging the crystal structure of the Fe_3O_4 core [33]. The broad peaks around 23° in Fe_3O_4@SiO_2, Fe_3O_4@SiO_2-glycine, and Fe_3O_4@SiO_2-malonic acid (Figure 2b–d, respectively) correspond to the amorphous shell of silica on the surface of the nanoparticles. In Figure 2c, the Fe_3O_4@SiO_2-glycine pattern, glycine-specific peaks appear at 29.85°, 30.45°, and 57.3° that correspond to (200), (111), and (302) reflections, respectively [34]. The (311) peak of the highest intensity was used to evaluate the diameter of Fe_3O_4 particles, approximately 21 nm. The patterns (COD 9006318) are

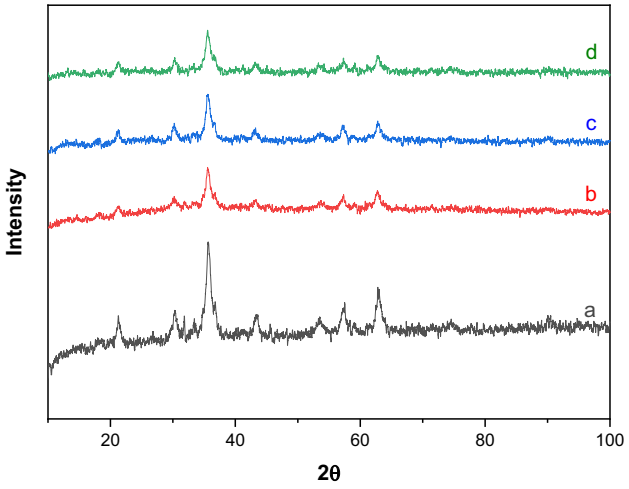

Figure 2: XRD diffraction patterns of (a) Fe_3O_4, (b) Fe_3O_4@SiO_2, (c) Fe_3O_4@SiO_2-glycine, and (d) Fe_3O_4@SiO_2-malonic acid nanoparticles.

consistent with the planes. Furthermore, diffractograms show no peak shifting upon coating and functionalization, indicating that the crystalline phase and the stability of magnetite nanoparticles were persevered. This further illustrates that the acid did not significantly affect the crystallinity or the crystal structure [35].

3.3 TEM analysis and particle size

The size and the morphology of the synthesized nanoparticles were characterized by TEM. TEM images of the prepared Fe_3O_4 and the Fe_3O_4@SiO_2 nanoparticles are shown in Figure 4. The as-prepared Fe_3O_4 nanoparticles exhibited spherical shapes and confirmed the increase in particle size after coating with SiO_2 as shown in Figure 3a. TEM micrograph (Figure 3b) showed spherical and rod-shaped particles with the SiO_2 layer after modification, and this layer was considered to consist of SiO_2, which is in good agreement with the previous FTIR and XRD results. The core (Fe_3O_4) and shell (SiO_4) structures of the nanoparticles were very clear in TEM images. The increase in particle size after coating with SiO_2 was further confirmed using TEM micrographs (ImageJ software), where the sizes of Fe_3O_4 and Fe_3O_4@SiO_2 nanoparticles were estimated to be 40.37 ± 2.97 nm and 53.20 ± 4.52 nm, respectively (Figure 3c).

DLS analysis was employed to confirm the particle size and hydrodynamic diameters and to monitor the aggregation behavior of the synthesized nanoparticles. The DLS particle size distribution results indicated that the synthesized Fe_3O_4 NPs and core-shell have size distribution with a monodispersity index (PDI) of 0.260 and monodispersity index 0.279, respectively. It is reported that PDI values greater than 0.7 indicate that the sample has a very broad size distribution [36]. The smaller value of the PDI index suggests that nucleation is fast compared to the particle growth, and also that the secondary nucleation step is absent. Therefore, systematic measurements of the average size and PDI of the synthesized NPs confirmed the long-term stability of the tested systems. It can be summarized that the synthesized nanoparticles were stable for at least 4 months [37]. The average particle size (diameter, nm) of the nanoparticle after being functionalized with glycine was 57.2496 nm and that with malonic acid was 229.433 nm. This could be explained by the difference in the number of atoms in malonic acid versus glycine [13]. DLS measurements indicated an increase in the mean diameter compared to TEM results due to the interference of the dispersant into the hydrodynamic diameter [38,39].

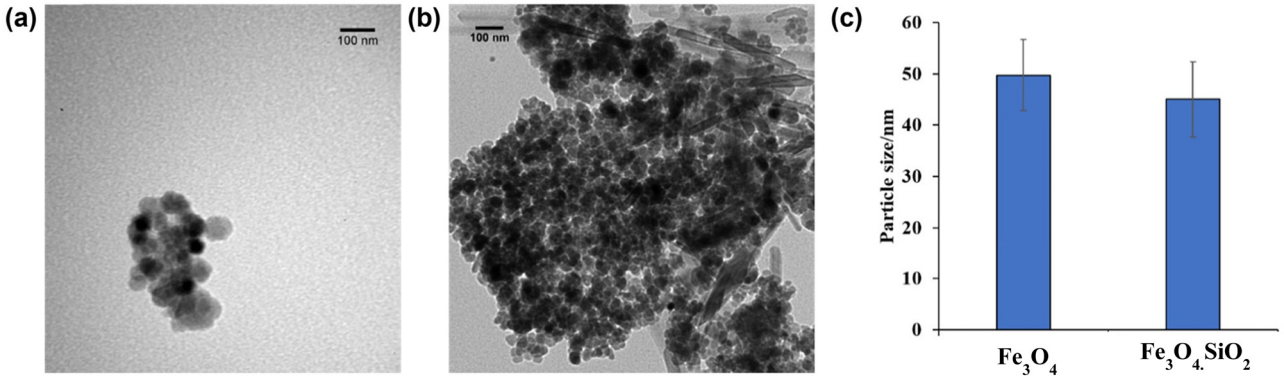

Figure 3: TEM images of (a) Fe_3O_4, (b) Fe_3O_4@SiO_2, and (c) nanoparticle size distribution of the synthesized nanoparticles.

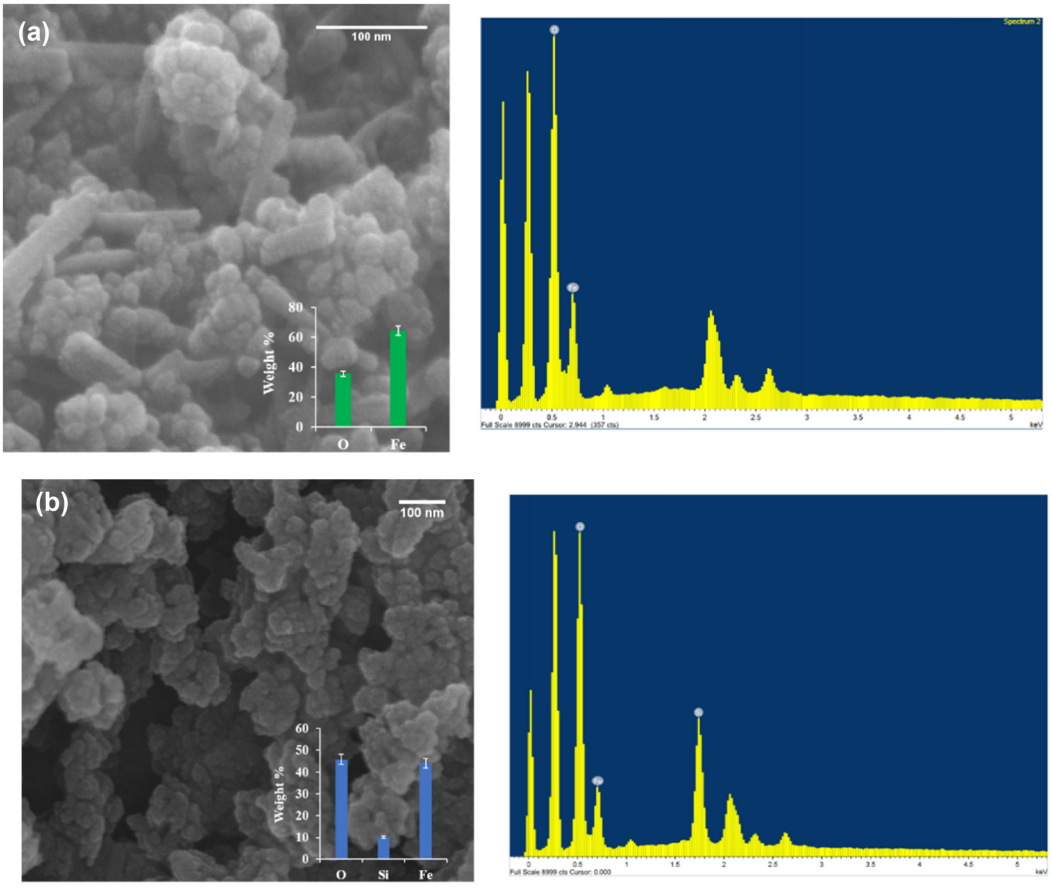

Figure 4: SEM images (left) and EDS (right) analysis for (a) Fe_3O_4 and (b) Fe_3O_4@SiO_2 nanoparticles.

3.4 SEM and EDS analysis

Figure 4 shows the SEM micrographs and the chemical composition of the synthesized nanoparticles. The synthesized Fe_3O_4 nanoparticles and Fe_3O_4@SiO_2, which were obtained via encapsulating magnetite nanoparticles in a shell of silica, are near spherical and possess a core/shell structure. EDS analysis demonstrated the chemical composition of the nanoparticles, and the percentage of Fe and O elements in Fe_3O_4 nanoparticles was 64.39% and 35.61%, respectively (Figure 4a). Moreover, the chemical composition of O, Si, and Fe in the Fe_3O_4 nanoparticles coated with SiO_2 was 45.8%, 10.09%, and 44.1%, respectively (Figure 4b). In the EDS spectrum, the presence of weak Si peaks and strong Fe peaks shows thin silica shell formation on the surface of Fe_3O_4 NPs [40].

The size of the nanoparticles was measured from the SEM micrograph using ImageJ software. The Fe_3O_4 and Fe_3O_4@SiO_2 particle size was 20.68 ± 0.75 nm and 75.16 ± 15.75 nm, respectively. The increased size of the Fe_3O_4 nanoparticles is explained by the SiO_2 coating. The nanoparticles exhibited a spherical shape, which was corresponding (Figure 4) to the TEM micrographs (Figure 3).

3.5 BET surface area analysis

The BET method was used to determine the specific surface area of the synthesized particles. The method is based on the adsorption of gas on the surface of the particles and measuring the amount of adsorbed gas at known pressure. By analyzing a known amount of particles, the specific surface area can be found. It has particular importance for adsorption, heterogeneous catalysis, and reactions on surfaces [41]. The BET method was carried out to estimate the specific surface area and porosity of the different synthesized particles. The pore size was determined to be about 1.59 nm and was nearly the same in both samples in terms of pore width and diameter. The BET surface area of the synthesized Fe_3O_4@SiO_2-glycine and Fe_3O_4@SiO_2-malonic acid was 104.8 and 26.15 m^2/g nm, respectively, which could be

related to their average particle size. The analysis in the present study determined that the smaller particle had a higher surface area [42–44]. The adsorption capacity of nanomagnetite relies on the availability of pore sites and the time taken for the adsorption process. The reduction in the pore size after adsorption could be attributed to blockage of the pores due to adsorption. Furthermore, the reduction in pore size after adsorption may be due to the blockage of the pores due to adsorption, which is in consensus with the findings of a previous study [45,46].

4 Conclusion

The key findings of the present study showed a successful synthesis of Fe_3O_4@SiO_2 nanoparticles by the co-precipitation method, followed by surface modification. The presence of functional groups was confirmed by FTIR analysis, and XRD patterns of samples confirmed the formation of Fe_3O_4, Fe_3O_4@SiO_2, and amorphous silica structures whose core-shell structure was indicated by TEM. Also, electron microscopy clearly demonstrated the impact of surface modification on morphology as well as the shape and the size of nanoparticles, as nanoparticles increased in size from about 20.68 ± 0.75 nm to 75.16 ± 15.75 nm after SiO_2 coating. After surface modification, a further increase in size was also observed in the Fe_3O_4@SiO_2-glycine and Fe_3O_4@SiO_2-malonic acid, to 57.2496 and 229.433 nm, respectively, where the surface area was increased to 104.8 and 26.15 m^2/g, respectively. Taken together, synthesized core-shell nanoparticles could provide a promising tool to be used for biomedical applications or for photocatalysis in the degradation of organic pollutants in wastewater water treatment.

Acknowledgments: The authors extend their appreciation to the Deputyship grant for Research & Innovation, "Ministry of Education in Saudi Arabia for funding this research work through the project number IFKSUHI-2020-135."

Funding information: This research project was supported by a grant from the "Research Center of the Female Scientific and Medical Colleges," Deanship of Scientific Research, King Saud University.

Author contributions: Seham S. Alterary: conceptualization, formal analysis, investigation, validation, resources, data curation, writing – original draft, writing – review and editing, visualization, supervision, funding acquisition, and project administration; Anfal AlKhamees: methodology, formal analysis, data curation, and writing – original draft.

Conflict of interest: The authors declare that there is no conflict of interest or state.

Data availability statement: All samples used in this research are available from the authors.

References

[1] Canaparo R, Foglietta F, Limongi T, Serpe L. Biomedical applications of reactive oxygen species generation by metal nanoparticles. Materials. 2021;14(1):53. doi: 10.3390/ma14010053.

[2] Cheraghi M, Lorestani B, Zandipak R, Sobhanardakani S. GO@ Fe_3O_4@ ZnO@ CS nanocomposite as a novel adsorbent for removal of doxorubicin hydrochloride from aqueous solutions. Toxin Rev. 2021;7:1–10. doi: 10.1080/15569543.2020.1839910.

[3] Ganapathe LS, Mohamed MA, Mohamad Yunus R, Berhanuddin DD. Magnetite (Fe_3O_4) nanoparticles in biomedical application: from synthesis to surface functionalisation. Magnetochemistry. 2020;6(4):68. doi: 10.3390/magnetochemistry6040068.

[4] Eskandari MJ, Hasanzadeh I. Size-controlled synthesis of Fe_3O_4 magnetic nanoparticles via an alternating magnetic field and ultrasonic-assisted chemical co-precipitation. Mater Sci Eng B. 2021;266(1):115050. doi: 10.1016/j.mseb.2021.115050.

[5] Samadi MS, Shokrollahi H, Zamanian A. The magnetic-field-assisted synthesis of the Co-ferrite nanoparticles via reverse co-precipitation and their magnetic and structural properties. Mater Chem Phys. 2018;215(15):355–9. doi: 10.1016/j.matchemphys.2018.05.067.

[6] Tizro N, Moniri E, Saeb K, Panahi HA, Ardakani SS. Preparation and application of grafted β-cyclodextrin/thermo-sensitive polymer onto modified Fe_3O_4@ SiO_2 nano-particles for fenitrothion elimination from aqueous solution. Microchem J. 2019;145(1):59–67. doi: 10.1016/j.microc.2018.09.005.

[7] van der Walt H, Chown L. Polysorbate stabilised Fe_3O_4 and Fe_3O_4@ Au nanoparticle synthesis and characterisation. Mater Today Proc. 2015 Jan 1;2(7):4081–9. doi: 10.1016/j.matpr.2015.08.038.

[8] Sobhanardakani S, Jafari A, Zandipak R, Meidanchi A. Removal of heavy metal (Hg(II) and Cr(VI)) ions from aqueous solutions using Fe_2O_3@ SiO_2 thin films as a novel adsorbent. Process Saf Environ Prot. 2018;120(1):348–57. doi: 10.1016/j.psep.2018.10.002.

[9] Chang Q, Zhu L, Yu C, Tang H. Synthesis and properties of magnetic and luminescent Fe_3O_4/SiO_2/Dye/SiO_2 nanoparticles. J Lumin. 2008;128:1890–5. doi: 10.1016/j.jlumin.2008.05.014.

[10] Sobhanardakani S, Zandipak R. Synthesis and application of TiO_2/SiO_2/Fe_3O_4 nanoparticles as novel adsorbent for removal of Cd(II), Hg(II) and Ni(II) ions from water samples. Clean

Technol Environ Policy. 2017;19:1913–25. doi: 10.1007/s10098-017-1374-5.
[11] Zandipak R, Sobhanardakani S. Novel mesoporous Fe_3O_4/SiO_2/CTAB–SiO_2 as an effective adsorbent for the removal of amoxicillin and tetracycline from water. Clean Technol Environ Policy. 2018;20(4):871–85. doi: 10.1007/s10098-018-1507-5.
[12] Farimani MH, Shahtahmasebi N, Roknabadi MR, Ghows N, Kazemi A. Study of structural and magnetic properties of superparamagnetic Fe_3O_4/SiO_2 core–shell nanocomposites synthesized with hydrophilic citrate-modified Fe_3O_4 seeds via a sol–gel approach. Physica E. 2013;1(53):207–16. doi: 10.1016/j.physe.2013.04.032.
[13] Sobhanardakani S, Jafari A, Zandipak R, Meidanchi A. Removal of heavy metal (Hg(II) and Cr(VI)) ions from aqueous solutions using Fe_2O_3@ SiO_2 thin films as a novel adsorbent. Process Saf Environ Prot. 2018;1(120):348–57. doi: 10.1016/j.psep.2018.10.002.
[14] Tizro N, Moniri E, Saeb K, Panahi HA, Ardakani SS. Preparation and application of grafted β-cyclodextrin/thermo-sensitive polymer onto modified Fe_3O_4@ SiO_2 nano-particles for fenitrothion elimination from aqueous solution. Microchem J. 2019;1(145):59–67. doi: 10.1016/j.microc.2018.09.005.
[15] Gemeay AH, Keshta BE, El-Sharkawy RG, Zaki AB. Chemical insight into the adsorption of reactive wool dyes onto amine-functionalized magnetite/silica core-shell from industrial wastewaters. Environ Sci Pollut R. 2019;9:1–8. doi: 10.1007/s11356-019-06530-y.
[16] López I, Garza-Tovar L, Adesuji ET, Sanchez-Dominguez M. Colloidal core-shell metal, metal oxide nanocrystals, and their applications. Colloidal metal oxide nanoparticles. India: Elsevier; 2020. p. 125–81. doi: 10.1016/B978-0-12-813357-6.00007-3.
[17] Agotegaray MA, Lassalle VL. Silica-coated magnetic nanoparticles: an insight into targeted drug delivery and toxicology. Switzerland: Springer; 2017. p. 4.
[18] Ahangaran F, Hassanzadeh A, Nouri S. Surface modification of Fe_3O_4@ SiO_2 microsphere by silane coupling agent. Int Nano Lett. 2013;3:23. doi: 10.1186/2228-5326-3-23.
[19] Kulkarni SA, Sawadh P, Palei PK. Synthesis and characterization of superparamagnetic Fe_3O_4@ SiO_2 nanoparticles. J Korean Chem Soc. 2014;58:100–4. doi: 10.5012/jkcs.2014.58.1.100.
[20] Tayebee R, Fattahi Abdizadeh M, Mohammadpour Amini M, Mollania N, Jalili Z, Akbarzadeh H. Fe_3O_4@ SiO_2-NH_2 as an efficient nanomagnetic carrier for controlled loading and release of acyclovir. Int J Nano Dimens. 2017;8:365–72, http://www.ijnd.ir/article_656346_6d8672cb773ae11ac80806ff50acbdae.pdfER
[21] Yuan Z, Xu R, Li J, Chen Y, Wu B, Feng J, et al. Biological responses to core–shell-structured Fe_3O_4@ SiO_2-NH_2 nanoparticles in rats by a nuclear magnetic resonance-based metabonomic strategy. Int J Nanomed. 2018;13:2447.
[22] Parvulescu VI, Coman SM. Core-magnetic composites catalysts for the valorization and up-grading of the renewable feedstocks: a mini review. CCAT. 2019;8(1):2–19.
[23] Asgari S, Fakhari Z, Berijani S. Synthesis and characterization of Fe_3O_4 magnetic nanoparticles coated with carboxymethyl chitosan grafted sodium methacrylate. J Nanostruct. 2014;4:55–63. doi: 10.7508/JNS.2014.01.007.
[24] Kang YS, Risbud S, Rabolt JF, Stroeve P. Synthesis and characterization of nanometer-size Fe_3O_4 and γ-Fe_2O_3 particles. Chem Mater. 1996;8:2209–11. doi: 10.1021/cm960157j.
[25] Peng S, Sun S. Synthesis and characterization of monodisperse hollow Fe_3O_4 nanoparticles. Angew Chem. 2007;119(22):4233–6. doi: 10.1002/ange.200700677.
[26] Saranya T, Parasuraman K, Anbarasu M, Balamurugan K. XRD, FT-IR and SEM study of magnetite (Fe_3O_4) nanoparticles prepared by hydrothermal method. Nano Vision. 2015;5:149–54, https://www.researchgate.net/publication/330511880
[27] Sun J, Zhou S, Hou P, Yang Y, Weng J, Li X, et al. Synthesis and characterization of biocompatible Fe_3O_4 nanoparticles. J Biomed Mater Res A. 2007;80:333–41. doi: 10.1002/jbm.a.30909.
[28] Du Q, Zhang W, Ma H, Zheng J, Zhou B, Li Y. Immobilized palladium on surface-modified Fe_3O_4/SiO_2 nanoparticles: as a magnetically separable and stable recyclable high-performance catalyst for Suzuki and Heck cross-coupling reactions. Tetrahedron. 2012;68:3577–84. doi: 10.1016/j.tet.2012.03.008.
[29] Hwang S, Umar A, Dar G, Kim S, Badran R. Synthesis and characterization of iron oxide nanoparticles for phenyl hydrazine sensor applications. Sensor Lett. 2014;12:97–101. doi: 10.1166/sl.2014.3224.
[30] Wang P, Wang N, Pang SF, Zhang YH. Hygroscopicity of internally mixed particles glycine/$NaNO_3$ studied by FTIR-ATR technique. J Aerosol Sci. 2018;116:25–33. doi: 10.1016/j.jaerosci.2017.11.013.
[31] Mekkapat S, Thong-On B, Rutnakornpituk B, Wichai U, Rutnakornpituk M. Magnetic core–bilayer shell complex of magnetite nanoparticle stabilized with mPEG–polyester amphiphilic block copolymer. J Nanopart Res. 2013;15:2051. doi: 10.1007/s11051-013-2051-1.
[32] Miñambres L, Méndez E, Sánchez MN, Castaño F, Basterretxea FJ. Water uptake of internally mixed ammonium sulfate and dicarboxylic acid particles probed by infrared spectroscopy. Atmos Environ. 2013;70:108–16. doi: 10.1016/j.atmosenv.2013.01.007.
[33] Shao X, Zhang Y, Pang SF, Zhang YH. Vacuum FTIR observation on hygroscopic properties and phase transition of malonic acid aerosols. Chem Phys. 2017;483:7–11. doi: 10.1016/j.chemphys.2016.11.001.
[34] Wei Y, Tian A, Li Y, Wang X, Cao B. A general chiral selector immobilized on silica magnetic microspheres for direct separation of racemates. J Mater Chem. 2012;22:8499–504. doi: 10.1039/C2JM30372H.
[35] Nawaz T, Zulfiqar S, Sarwar MI, Iqbal M. Synthesis of diglycolic acid functionalized core-shell silica coated Fe_3O_4 nanomaterials for magnetic extraction of Pb(II) and Cr(VI) ions. Sci Rep. 2020;10(1):1–3. doi: 10.1038/s41598-020-67168-2.
[36] Pham XH, Hahm E, Kim HM, Son BS, Jo A, An J, et al. Silica-coated magnetic iron oxide nanoparticles grafted onto graphene oxide for protein isolation. Nanomaterials. 2020;10(1):117. doi: 10.3390/nano10010117.
[37] Szczęch M, Szczepanowicz K. Polymeric core-shell nanoparticles prepared by spontaneous emulsification solvent evaporation and functionalized by the layer-by-layer method. Nanomaterials. 2020;10(3):496. doi: 10.3390/nano10030496.
[38] Souza TG, Ciminelli VS, Mohallem ND. A comparison of TEM and DLS methods to characterize size distribution of ceramic

nanoparticles. J Phys Conf Ser. 2016;733(1):012039. doi: 10.1088/1742-6596/733/1/012039.
[39] Shi Y. Functionalized silica nanostructures: degradation pathways and biomedical application from 2D to 3D. PhD thesis. Paris: Sorbonne Université; 2018.
[40] Ahamed SZA, Dillip G, Raghavaiah P, Mallikarjuna K, Raju BDP. Spectroscopic and thermal studies of γ-glycine crystal grown from potassium bromide for optoelectronic applications. Arab J Chem. 2013;6:429–33. doi: 10.1016/j.arabjc.2011.06.006.
[41] Wypych G. 13 – Analytical techniques useful in foaming. In: Wypych G, editor. Handbook of foaming and blowing agents. Ontario: ChemTec Publishing; 2017. p. 219–25. doi: 10.1016/B978-1-895198-99-7.50015.
[42] Zhang GY, Feng Y, Xu YY, Gao DZ, Sun YQ. Controlled synthesis of mesoporous α-Fe_2O_3 nanorods and visible light photocatalytic property. Mater Res Bull. 2012;47:625–30. doi: 10.1016/j.materresbull.2011.12.032.
[43] Zheng Y, Cheng Y, Wang Y, Bao F, Zhou L, Wei X, et al. Quasicubic -Fe_2O_3 nanoparticles with excellent catalytic performance. J Phys Chem B. 2006;110:3093–7. doi: 10.1021/jp056617q.
[44] Ruby P, Vipul S, Umar F, Meryam S, Abul K, Abdullah GA, et al. One pot synthesis and surface modification of mesoporous iron oxide nanoparticles. Nano-Struct Nano-Objects. 2019;19:100343. doi: 10.1016/j.nanoso.2019.100343.
[45] Demetriou A, Pashalidis I. Adsorption of boron on iron-oxide in aqueous solutions. Desalin Water Treat. 2012;37(1–3):315–20. doi: 10.1080/19443994.2012.661288.
[46] Abba MU, Che Man H, Azis S, Idris AI, Hazwan Hamzah M, Abdulsalam M. Synthesis of nano-magnetite from industrial mill chips for the application of boron removal: characterization and adsorption efficacy. Int J Environ Res Public Health. 2021;18(4):1400. doi: 10.3390/ijerph18041400.